Interactions between water and 1-butyl-1-methylpyrrolidinium ionic liquids

Tatiana A. Fadeeval, Pascale Husson, Jessalyn A.DeVine, Margarida F. Costa Gomes, Steven G. Greenbaum, and Edward W. Castner Jt: b)

We report experimental results on the diffusivity of water in two ionic liquids obtained using the pulsed-gradient spin-echo NMR method. Both ionic liquids have the same cation, 1-butyl-1-methylpyrrolidinium, but different trifluoromethyl-containing anions. One has a strongly hydrophobic anion, bis(trifluoromethylsulfonyl)amide, while the second has a hydrophilic anion, trifluoromethylsulfonate. Transport of water in these ionic liquids is much faster than would be predicted from hydrodynamic laws, indicating that the neutral water molecules experience a very different friction than the anions and cations at the molecular level. Temperature-dependent viscosities, conductivities and densities are reported as a function of water concentration to further analyze the properties of the ionic liquid-water mixtures. These results on the properties of water in ionic liquids should be of interest to researchers in diverse areas ranging from separations, solubilizing biomass and energy technologies.

Keywords: ionic liquid, water, diffusivity, transport, viscosity

INTRODUCTION

Applications of ionic liquids (ILs) to significant problems in energy sciences and biomolecular studies require an understanding of how water interacts with the ionic species. Hydrogen fuel cells with ionic liquids show great promise, where the end product of the electrochemical reaction is water.^{1,2} Even trace amounts of water for ILs applications such as lithium batteries can have deleterious effects on performance. Photo-catalytic water splitting with increased efficiency and decreased overpotentials may become possible with the use of ILs. Agueous biphasic systems are increasingly used for complex separations tasks³ One of the more important applications of aqueous-IL separations is to use ILs for solubilizing biomass or effecting enzymatic catalysis transformations, where the role of water will be crucial.^{4,5} ILs with added water show distinctly non-hydrodynamic behavior, so careful consideration of the thermodynamics. transport, and interactions of the IL anions and cations together with the added water is needed.

While ILs that have sufficiently hydrophobic anions and cations can phase separate from water, even these hydrophobic ILs still have significant mole fractions of water at the solubility limits. ⁶ In most ionic liquids, the interactions between water and the ions are dominated by anion-water interactions, as discussed by Cammarata.

A number of researchershave applied NMR methods to understand the properties of ILs, 10-12 including ILs with dissolved water. 13-15 Pulsed-gradient spin-echo (PG-SE) NMR spectroscopy provides a direct means for detecting diffusivity of the molecular ions and solute molecules. 16-18 Other methods make use of the nuclear Overhauser effect to study the specific interactions between spins on neighboring molecules or molecular ions. 19-22 In a study of water in an IL or a mixture of an IL with the ionic polymer Nafion, Hou, et al. showed that water diffusivity was up to 10 times faster than the larger anions in the 1-ethyl-3-methylimidazolium (emim⁺) BF₄ water-IL mixtures. When the diffusivity ratio was considered between the neutral and the anion in a Nafion membrane. the water diffusivity was as much as 60 times larger than for the BF₄ anion. 14 Thus, predictions based on the Stokes-

¹⁾ Department of Chemistry and Chemical Biology, Rutgers, The State University of New Jersey, Piscataway, NJ 08854

²⁾ CNRS, UMR 6296, Institut de Chimie de Clermont-Ferrand, BP 80026, F-63171 Aubi`ere and Clermont Universit´e, Universit´e Blaise Pascal, Institut de Chimie de Clermont-Ferrand, BP 10448, F-63000 Clermont-Ferrand, France

³⁾ CNRS, UMR 6296, Institut de Chimie de Clermont-Ferrand, BP 80026, F-63171 Aubi`ere, France

⁴⁾ Department of Physics and Astronomy, Hunter College, CUNY, New York, NY 10065

et al. 7 Significant effort is expended by the IL research community to ensure that physical and chemical properties of ILs were measured on dry samples, since water is known to be rapidly absorbed through exposure to atmospheric moisture.8 Characterization of water in ionic liquids is most commonly done by means of a Coulometric Karl Fischer titration, which is destructive to the sample. so alternative means of characterizing water have been developed using near-IR spectroscopy.8 As surface science experiments progressed on ILs,mass spectroscopic studies of ILs in ultra-high vacuum (UHV) conditions revealed that even so-called 'dry' samples still contained significant quantities of water from the perspective of electrochemists and surface scientists. However, multiple distillation passes in UHV conditions permit removal of all detectable water.9

a) present address: Department of Chemistry, College of Chemistry, University of California at Berkeley, Berkeley, CA 94720

b) Electronic mail: ed.castner@rutgers.edu

Einstein hydrodynamic law will not apply for the case of water in ILs or in IL polyelectrolyte membranes. Moreno, *et al.* have characterized two ILs with the OTf⁻ anion, paired with the Pyrr ⁺₁₄ and the 1-methyl-1-methoxyethylpyrrolidinium cations. ¹⁵ The structure of water-IL solutions was studied using molecular simulation methods by Bernardes, *et al.*²³ where the authors reported the aggregation properties of either water or ions over the full range of concentrations of water with the IL 1-ethyl-3-methylimidazolium ethylsulfate.

We have studied water in two common ionic liguids using an array of methods that includes NMR and vibrational spectroscopy, viscosity, conductivity, and density measurements. The ILs studied, 1-butyl-1-methylpyrrolidinium bis(trifluoromethylsulfonyl)amide (Pyrr ⁺₁₄/NTf ⁻₂) and 1-butyl-1-methylpyrrolidinium trifluoromethylsulfonate (Pyrr ⁺₁₄/OTf ⁻), are shown in Fig. 1. These ILs share the same non-aromatic Pyrr ⁺₁₄ cation, but they have different anions: hydrophobic NTf 2 and more water-miscible OTf -. Fig. 1 presents the structure of the anions and the cation. The Pyrr $^+_{14}/NTf$ $^-_2$ is less than half as viscous as Pyrr $^+_{14}/OTf$ $^-$; the viscosities at 298.2 K are 78.4 cP and 168 cP, respectively. The decreased viscosity for NT relative to OTf - anion ILs results from several factors. These include the increased size and intramolecular flexibility of NTf 2 relative to OTf $^-$ and the presence of two meta-stable cisoid and transoid conformers for NTf $_2^-$. 15,19,24,25

FIG. 1. Structures of the ionic liquid ions. 1-butyl-1-methylpyrrolidinium cation (Pyrr $_{14}^+$, black), bis(trifluoromethylsulfonyl)amide anion (NTf $_2^-$, blue), and trifluoromethylsulfonate (OTf $_-$, red).

We present a comparison of methods used for non-destructive characterization of small quantities of water in ILs. These methods were used together with the more common Karl-Fischer coulometric titrations to prepare IL samples with precisely known water contents. Experiments on these water-IL mixtures included bulk ther-modynamic measurements of density, viscosity and conductivity as a function of temperature. The individual self-diffusion coefficients for water, anions and the cation in these IL-water mixtures are obtained from pulsed-gradient spin echo (PG-SE) NMR experiments. Comparing the self-diffusivities from PG-SE NMR experiments with the bulk conductivities permits evaluation of the degree of ionicity in the solutions.

EXPERIMENTAL METHODS

Materials

The Pyrr $^+_{14}/{\rm NTf}~^-_2$ and Pyrr $^+_{14}/{\rm OTf}~^-$ ILs were purchased from Merck/EMD or IoLiTec. IoLiTec samples IoLiTec samples were used for viscosity, density and conductivity measurements. The ¹H NMR spectra showed the ence of methylene chloride CH₂Cl₂ in ILs bought from Merck/EMD and presence of water for ILs from both vendors. ILs were placed under vacuum for 48 hours to remove these impurities. To prepare samples of a particular water concentration, we added water to the IL and stirred for 10 hours to ensure homogeneity of the solution. The mixtures of the ionic liquids with water were prepared gravimetrically and the concentrations were also verified by Karl-Fisher (KF) titration before and after each measurement. The overall uncertainty in the composition of the mixtures expressed in mole fraction was estimated to be \pm 0.002.

Water concentrations in the ionic liquids were determined by coulometric Karl-Fisher titration using a Denver Instrument 260 Titration controller or a Mettler-Toledo DL31 instrument. The Hydranal-Coulomat CG reagent was used as a catholyte, and Hydranal-Coulomat AG reagent was used as an analyteThe lower sensitivity limit for the method is $\approx 2\mu {\rm g}$ or 0.5 ppm by mass water. The water content of each sample was measured twice. Sample volumes ranged from 0.5 to 1.5 mL depending on the desired water concentration. One sample for each liquid was kept as dry as possible: Pyrr $^+_{14}/{\rm NTf}\,^-_2$ - with $X_{H_2O} = 0.00023$ and Pyrr $^+_{14}/{\rm OTf}\,^ X_{H_2O} = 0.00065$, where X_{H_2O} is the mole fraction of water in the ionic liquid.

Density, viscosity and conductivity measurements

The density was measured using a vibrating-tube densimeter (DMA 5000M) following procedures described previously. The precision of the density measurement is $\pm\,5\times10^{-5}\,$ g cm $^{-3}$. The viscosity was measured using a microviscometer (Lovis 2000ME, Anton Paar) based on the falling-ball principle. A capillary tube with a nominal diameter of 1.8 mm was used. The viscometer was calibrated using a viscosity standard (APN26 oil, Anton Paar). The temperature of the apparatus was controlled to within $\pm 0.01\,$ K and the uncertainty in the viscosities are $\pm 2\%$.

The conductivity ionic was estimated impedancemetry using an impedance analyzer (7260, Material Mates) and a sealed conductivity cell in borosilicate glass equipped with two platinum electrodes (Material Mates). The calibration constant of the cell was determined as a function of temperature using aqueous KCl solutions. A drive voltage of 100 mV was applied to the cell and the resistance of the solution was measured as a function of the frequency (varying typically from 100 Hz to 100 kHz). The temperature of the cell was controlled within ±0.1 K. The uncertainty of the conductivity measurements is ±1% and the uncertainty for the molar conductivities is ±2%.

NMR sample preparation

To avoid gas exchange and to prevent temperature gradients that could lead to convection in the IL/water mixture, samples were flame sealed in a small capsule immediately after determination of water content. The capsules used were typically 45 mm long. The outer and inner diameters were 3.5 and 3.13 mm, respectively. The amount of liquid in the capsule was adjusted so that the length of the sample did not exceed 30 mm. Both a reduced sample length and diameter help to minimize convection effects on the signal. The capsule was placed inside a 5 mm outer diameter NMR tube filled with Krytox oil (a hydrogen-free branched perfluoroether from DuPont) that served as a liquid bath to eliminate any temperature gradient along the sample.

Spectroscopic determination of water content in ILs

We have used both 1H NMR and FT-IR spectroscopy to measure the water content in ILs. We have found that measuring the absorbance of the water $\nu_2 + \nu_3$ vibrational combination band observed near 5,250 cm 1 is more sensitive than using 1H NMR.

After drying, IL samples used for spectroscopic determination of water content were handled under a nitrogen atmosphere in a glove tent (Captair). An aliquot of each ionic liquid sample was used for KF analysis to obtain a standard water determination of water content. The samples used for the dry-IL spectra were analyzed using Karl Fischer and had water concentrations in the range between 2–8 ppm by mass.

A 5-mm path length IR quartz cuvette (NSG Precision Cells) was filled and sealed with a Teflon stopper. The cuvette was removed from isolation and placed in the sample chamber of a Nicolet iS-10 FT-IR spectrometer with an MCT detector and 8 cm ⁻¹ spectral resolution. The sample chamber had been purged with high-purity argon or nitrogen gas to minimize atmospheric water. 32 scans were recorded for each near-IR spectrum, requiring about 3 minutes for data acquisition. The 1 cm optical path gives a maximum absorbance from the IL in the range from 0.7 to 1.1, so careful baseline subtraction of a dry IL spectrum is required for determination of lowest water concentrations. The water vibrational lineshapes are a strong function of the choice of anion, with nearly a factor of two variation in the linewidth (fwhm) seen between ILs having the same cation but different anions.

Fig. 2 demonstrates the detection limit for water based on a carefully baseline-corrected measurement of the $v_2 + v_3$ combination band of water. The baseline correction relies on a smoothly varying absorbance for the ionic liquid that is observed to be about 0.18 for this spectral range for the spectrum shown in Fig. 2. Using a standard 'IR-quartz' sealed cuvette with a 1 cm optical path in an entry-level FT-IR instrument, with 32 scans and 8 cm¹ spectral resolution, the spectra in Fig. 2 are obtained (top), and following baseline correction, these spectra are shown in Fig. 2. The inset in Fig. 2

shows the spectrum for the lowest concentrations that we could reproducibly prepare and measure by FT-IR, NMR and Karl-Fischer titration, which was 59 ppm for the measured trace shown in blue. Raw and corrected spectra for $\mbox{Pyrr}_{14}^+/\mbox{NTf}_2^-$, 1-butyl-3-methylimidazolium (bmim $^+$)/NTf $_2^-$, and bmim $^+$ /PF $_6^-$ are provided in the supplementary information. 28

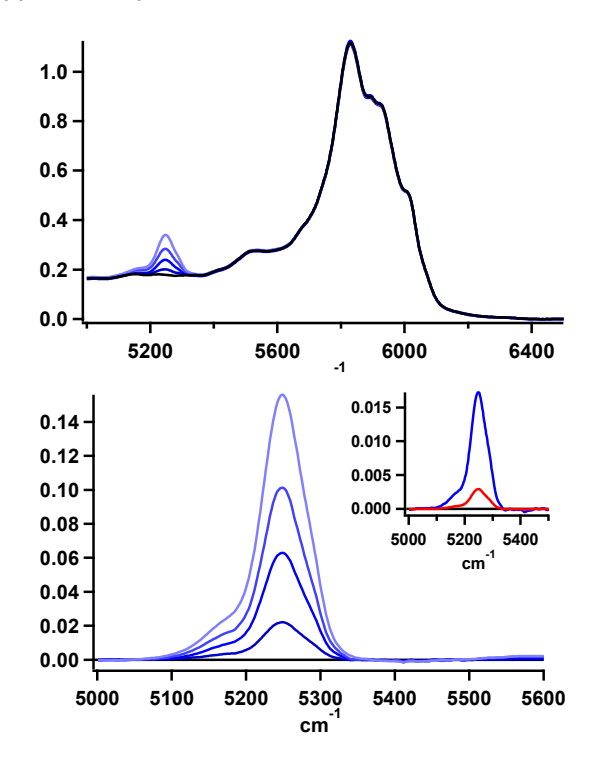


FIG. 2. Near infrared absorbance spectra of ionic liquids for several water concentrations. (top) Pyrr $^{+}_{14}/NTf$ $^{-}_{2}$ with lowest concentration, 79, 311, 571, and 773 ppm of water by mass. (bottom) Baseline-subtracted absorbance spectra of the water $\nu_2 + \nu_3$ transition for the same water concentrations in Pyrr $^{+}_{14}/NTf$ $^{-}_{2}$. The inset graph shows a low-concentration sample (blue, 59 ppm) and the same spectrum divided by 5.9, to illustrate an estimated spectrum for 10-ppm sample water content (red).

To estimate the limit of detection for these samples, we provide the same spectrum scaled by 5.9 in order to compare the intensity for a spectral intensity corresponding to a 10 ppm water concentration with the noise floor for the experiment with 32 scans. Intensities corresponding to 10 ppm are well above the detection limit by visual inspection, with no need for sophisticated spectral analysis. It should be possible to reduce the detection limit to below 1-2 ppm water concentration by using additional scans, higher spectral resolution, additional drying of the ionic liquid in ultra-high vacuum and application of numerical methods to spectral analysis. We have thus shown that any modern FT-IR instrument can be used to determine the water content in an IL sample non-destructively with similar levels of sensitivity to the commonly used KF titration method.

NMR spectroscopy is a method commonly used to investigate many aspects of the physical chemistry of ionic

liquids.²⁹ In particular, ¹H-NMR signals are very sensitive to the interactions between the ILs and absorbed water. In our efforts to develop non-destructive methods of water quantification in ionic liquids, we also investigated the possibility of using ¹H NMR spectroscopy.

One of the complications of using NMR to investigate water in ionic liquids is the temperature-dependence of the water chemical shift. It is well known that bulk water has a significant change in chemical shift with temperature; the ¹H peak of HDO shifts by about 1.0 ppm over the liquid temperature range of 100 $^{\circ}$ C. 30 In addition to undergoing significant changes to the chemical shift with temperature, the position of the ¹H peak for water in ILs is also strongly concentration dependent. Fadeeva previously studied the concentration-dependence of the chemical shift in Pyrr ⁺₁₄/NTf ⁻₂, and found that for increasing concentrations the water peak moves downfield.31 This change in the ¹H chemical shift with concentration provides an additional complication in the use of NMR for water determination, as the peak may shift so that it is completely obscured by a much more intense peak from the IL cation or anion. Accounting for these complications permits us to use routine ¹H NMR spectroscopy to determine water content to a level of about 50 ppm, and in special cases, to below 20 ppm.

Diffusivity from NMR pulsed-gradient spin-echo experiments

Self-diffusion coefficients were measured using the PG-SE method. ^{16,17} The specific pulse sequence use was the Bipolar Pulse Pair Stimulated Echo Experiment (DBPPSTE) pulse sequence described by Wu, Chen and Johnson. ¹⁸ The intensity of the PG-SE signal was measured as a function of incremental gradient strength using an array of 12-15 values of the gradient field strength *g*. The self-diffusion coefficient *D* is obtained by fitting the spin echo intensities to the following equation:

$$I_g = I_0 \exp - (y\delta g)^2 D \quad \Delta - \frac{\delta}{3} \quad .$$
 (1)

where I_g is the intensity of the signal, I_0 is the intensity of the signal at g = 0, y is gyromagnetic constant, δ is duration of the gradient pulse (s), Δ is diffusion delay (s), and D is the diffusivity.

All PG-SE measurements were performed using a narrow bore Varian DirectDrive spectrometer operating at a ^1H resonance frequency of 400 MHz. Measurements of ^1H and ^{19}F spectra and T_1 and T_2 relaxation times were performed using a Varian Auto-X Dual Broadband probe. The field gradient in the PG-SE experiments was generated using a Doty Scientific model 16-38 diffusion probe and a Highlander gradient amplifier. Samples were equilibrated for 15 min after each temperature change. Calibrations were done by recording the chemical shift vs. temperature for methanol (below ambient) and ethylene glycol (above ambient), as described by Claridge, *et al.* 27

The cation diffusivity was obtained by fitting the ¹H

PG-SE signal intensity $\frac{l_g}{l_0}$ to Eq. 1 as a function of g using Varian vNMRj software. The diffusivity of the seven different ¹H peaks of Pyrr ⁺₁₄ varied only insignificantly. Experimental parameters included a gradient pulse duration of δ = 2 ms. The diffusion time delay Δ is normally set to be significantly less than the T_{-1} relaxation time in order to avoid signal attenuation resulting from spinlattice relaxation. Measured values of T varied from 0.5 to 1 s. so the value of Δ was chosen to be 70 ms. To ensure that convection was not affecting the measured diffusivity, experiments were run for a range of Δ values: The intensity of the PG-SE signal has a convection term that depends on Δ . ²⁷ To determine whether convection affects the measured values of D, the PG-SE sequence was measured for three different diffusion delays: Δ = 50, 70 and 100 ms. Test measurements were done at 318 K, the highest temperature for which we recorded diffusivity data. From these precautions, we determined that no sign of convection was observed. To obtain the best possible signal, the probe was retuned following each temperature change. Calibration of the $\frac{\pi}{2}$ -pulse width pw also was conducted following each temperature change. The intensity of the spin echo signal was measured as a function of the gradient field strength q, which was varied from 5 to 350 G/cm (0.05 - 3.5 T/m). The gradient strength array was arranged so that the intensity of the PG-SE signal for the largest applied field gradient had an intensity of approximately 25% of the maximum signal.

Some peaks were found to exhibit better reproducibility than others. Several experiments were repeated to determine the ^1H peak with smallest standard deviation. The ^1H peak at 2.2 ppm resulting from the 3- and 4- positions of the pyrrolidinium ring, labeled as peak '4' in Fig. 3, shows the smallest variance. Therefore, all cation diffusivities reported are from this peak. Neither the NTf $^-_2$ nor the OTf $^-$ anions have any hydrogen atoms, so the diffusivities of the anions were determined from ^{19}F PG-SE experiments in the same way as \mathcal{D}_{ation} was obtained from ^{1}H PG-SE experiment. The anions have a single ^{19}F peak arising from the trifluoromethyl groups.

The chemical shift of water in ILs, δ_{H2O} , varies strongly with the water concentration, the nature of the anion, and the sample temperature. The diffusivities for certain chemical shifts are bimodal, with one component arising from water diffusivity and a second, slower component arising from the cation diffusivity. Thus, a double-exponential fit of the spin echo intensity as a function of g is used to determine the two diffusivities, as described by Menjoge, et al.

RESULTS AND DISCUSSION

Temperature-dependent density, viscosity and conductivity of the water-ionic liquid solutions

The densities of the pure ionic liquids were measured as a function of temperature from 298 to 333 K (Table I). A linear variation of this property was observed as a

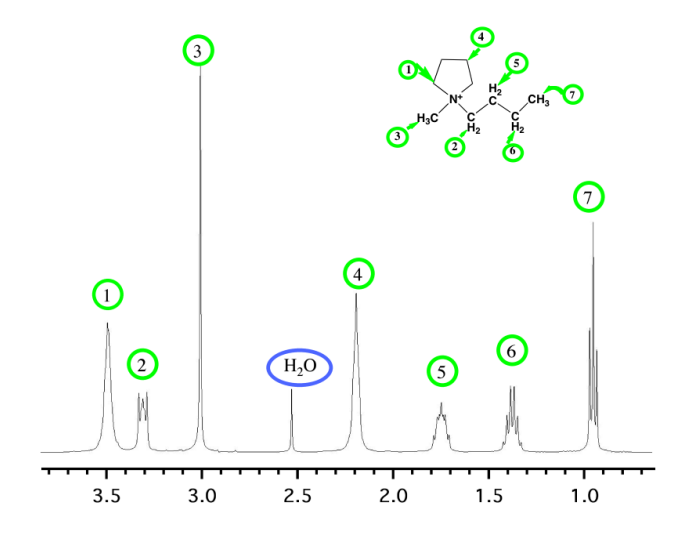


FIG. 3. 1 H NMR spectrum of Pyrr $^{+}_{14}$ /NTf $^{-}_{2}$ measured using the Doty model 16-38 probe.

function of temperature and fit to

$$\rho = A + B \times T, \tag{2}$$

where the units for ρ are kg-m⁻³, the temperature T in units of $^{\circ}$ C, the parameters are A=1.41718×10 3 and 1.27040×10 3 kg-m⁻³ and B= -0.876913 and -0.720634 kg-m⁻³ -K⁻¹. The standard deviation between experimental and calculated densities are 4×10 5 and 3×10 $^{-5}$ for Pyrr $_{14}^{+}$ /NTf $_{2}^{-}$ and Pyrr $_{14}^{+}$ /OTf $_{2}^{-}$, respectively. These experimental data are compared with temperature-dependent density data presented in literature and found to agree to 0.1%; this comparison is given in the supplementary information. 28

TABLE I. Temperature-dependent densities for the 'dry' ILs. The uncertainties are ± 0.01 K in temperature and $\pm 5 \times 10^{-5}$ gm cm⁻³ in density.

| | Pyrr ⁺ ₁₄ /NTf ⁻ ₂ | Pyrr ⁺ ₁₄ /OTf ⁻ |
|--------|--|---|
| T (K) | $ ho$ (g cm $^{-3}$) | $ ho$ (g cm $^{-3}$) |
| 298.15 | 1.39530 | 1.25239 |
| 303.15 | 1.39087 | 1.24881 |
| 313.15 | 1.38205 | 1.24154 |
| 323.15 | 1.37330 | 1.23434 |
| 333.15 | 1.36461 | 1.22720 |

Pure Pyrr ⁺₁₄/NTf ⁻₂ is two times less viscous than Pyrr ⁺₁₄/OTf ⁻ (78 vs. 168 mPa-s at 298 K). It was also observed on imidazolium-based ionic liquids that the presence of the anion NT½ lowers the viscosity of the liquid. For both ionic liquids, an important decrease of the viscosity is observed when increasing temperature, as predicted by Eq. 3, where the adjustable parameters are given in Table II. The viscosities are compared with all other available literature values in the supplementary information, ²⁸ and these data present an average deviation of less than 2% which can be considered as the

global uncertainty of our viscosity measurement. For $Pyrr_{14}^+/OTf^-$ an average relative deviation of 0.3% is observed with the data of Gacino, *et al.* ³²

TABLE II. Temperature-dependent viscosity parameters η_0 , B and T_0 obtained from fits to the VFT model (eq. 3) and the Arrhenius activation energy E_a ; the estimated uncertainty in E_a is ± 1 kJ mol $^{-1}$.

| X _{H 2} O | η_0 (mPa-s) | B (K) T | ₀ (K) E | a (kJ mol ⁻¹) |
|----------------------------|------------------|---------|--------------------|---------------------------|
| Pyrr + /OTf - | | | | |
| 0.001 | 0.16691 | 891.94 | 169.16 | 34.84 |
| 0.048 | 0.13526 | 938.45 | 163.65 | 34.00 |
| 0.117 | 0.16546 | 861.81 | 165.38 | 31.95 |
| 0.174 | 0.17162 | 831.93 | 165.86 | 31.06 |
| Pyrr $_{14}^+$ /NTf $_2^-$ | | | | |
| 0.002 | 0.16173 | 826.17 | 164.54 | 30.32 |
| 0.056 | 0.18985 | 772.13 | 167.38 | 29.44 |
| 0.106 | 0.32629 | 590.71 | 182.84 | 28.17 |
| 0.185 | 0.17061 | 761.17 | 164.24 | 27.85 |

The presence of water drastically decreases the viscosity of both ionic liquids. For example, for x_{H_2O} =0.17 in the IL, the viscosity is decreased by 45% and 36% relative to neat Pyrr $_{14}^+$ /OTf $_-^-$ and Pyrr $_{14}^+$ /OTf $_-^-$, respectively. Temperature also has a dramatic effect on viscosity; for example a temperature increase of 35 K reduces the viscosity by a factor 4 in both ionic liquids.

The viscosities measured from 298 to 333 K for the pure ionic liquids and their mixtures with water are presented in Tables III and IV and Fig. 4. As is normally observed for ionic liquids, ^{6,10,11,33–39} the Vogel-Fulcher-Tammann (VFT) model, given by the following equation,

$$\eta = \eta_0 \exp \frac{B}{T - T_0} \tag{3}$$

provides a superior fit to the temperature-dependent viscosity than the Arrhenius model, so the VFT parameters in Table II are used to calculate and extrapolate viscosities for other temperatures to high accuracy. However, the Arrhenius fits, while less good, are still useful for considering the activation energy for viscous flow for the higher temperatures we have studied here. We estimate that the uncertainty in the viscosity activation enthalpy E_a is ±1 kJ mol $^{-1}$. The activation enthalpy E_a is significantly higher for Pyrr $^+_{14}$ /OTf $^-_{2}$ though both decrease by up to 10% on the addition of increasing amounts water.

The ionic conductivities of the pure ionic liquids and their mixtures with water were measured from 298 to 333 K, and the data were fit to Eq. 4. The fit parameters were κ_0 115.82 and 248.06 S- \vec{m} , B^0 =-875.75 and -1,081.80 K, T_0^0 =152.99 and 146.59 K, with standard errors of 7 ×10⁴ and 5×10⁻⁷ for Pyrr $^+_{14}$ /NTf $^-_2$ and Pyrr $^+_{14}$ /OTf $^-$, respectively. Higher conductivity is observed for Pyrr $^+_{14}$ /NTf $^-_2$

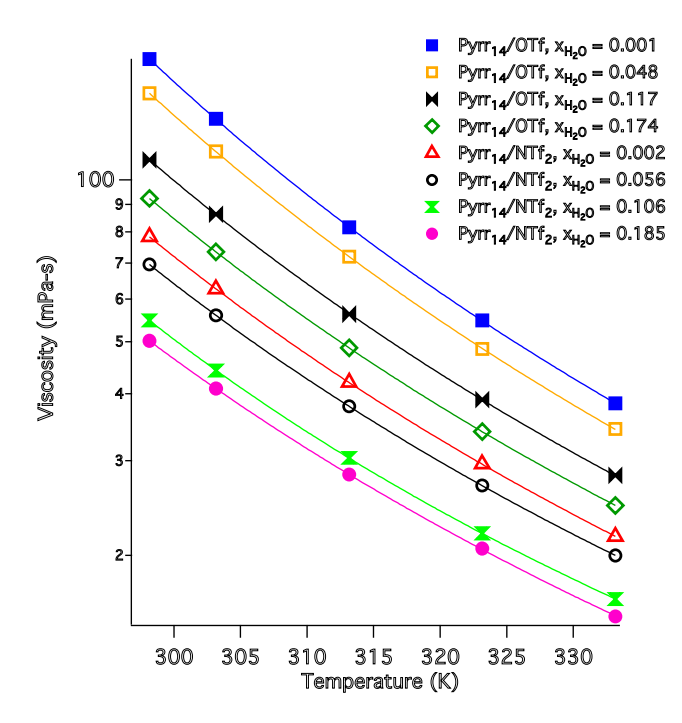


FIG. 4. Shear viscosity plotted vs. temperature for $Pyrr_{14}^+/OTf^-$ and $Pyrr_{14}^+/NTf_2^-$ for several water concentrations. Solid lines are fits to the VFT model (eq. 3).

than for Pyrr $^+_{14}$ /OTf $^-$ largely because of the lower viscosity for the former. For both ionic liquids, the conductivity increases strongly for increasing temperature, following the VFT equation

$$\kappa = \kappa_0 \exp \frac{B^0}{T - T_0^0} \tag{4}$$

No conductivity data for Pyrr $_{14}^+/{\rm OTf}^-$ were found in literature for comparison. For Pyrr $_{14}^+/{\rm NTf}_2^-$, the ionic conductivity measured in the present work deviates by 1% from the data of Vranes *et al.*,40 Harris, *et al.*41 and Tokuda, *et al.*11 This value can be considered as the global uncertainty on the conductivity measurement.

As the addition of water decreases the viscosity of the liquid, it also increases its ionic conductivity. As already observed for the viscosity, temperature has a more important on this transport property compared to the addition of water. An increase of the ionic conductivity is observed when increasing temperature.

¹H NMR spectrum of Pyrr + /NTf - and Pyrr+ /OTf -

Both ILs have the same cation Pyrr $^+_{14}$ / and protonless anion and, because of that, they have the same 1 H spectrum. The typical 1 H spectrum of Pyrr $^+_{14}$ /NTf $^-_2$ containing water is shown in Fig. 3. The peak labeled '7' originates from the protons of the terminal methyl group on the butyl chain. The peaks '5' and '6' are assigned to the protons of methylene groups on the butyl chain. The peak '2' is assigned to the methylene group attached to the nitrogen. Peak '3' is assigned to the 1-methyl protons. Peak '1' signals are from the 2- and 5-pyrrolidinium

TABLE III. Temperature-dependent viscosities (η), ionic conductivities (κ), and molar conductivities (Λ $_{imp}$) for mixtures of Pyrr $_{14}^+$ /NTf $_{2}^-$ and water for the different mole fractions of water, χ_{H_2O} . The uncertainties in T $_{visc}$ and T $_{cond}$ are \pm 0.01 and 0.1 K, respectively. The uncertainties are viscosity: \pm 2%; conductivity: \pm 1%; and molar conductivity: \pm 2%.

| Tvisc | (K) η (| (mPa-s) | T _{cond} (K) | κ (S-m ⁻¹) | $\Lambda_{imp} \times 10^4$ |
|---------------------------|---------|---------|-----------------------|------------------------|-----------------------------|
| | | | | | $(S-m^2-mol^{-1})$ |
| | | | $X_{H_2O} = 0.00$ | 2 | |
| 298 | 3.15 | 78.4 | 298.2 | 0.28 | 0.84 |
| 303 | 3.15 | 62.7 | 303.1 | 0.34 | 1.03 |
| 313 | 3.15 | 42.0 | 313.2 | 0.49 | 1.49 |
| 323 | 3.15 | 29.6 | 323.2 | 0.68 | 2.07 |
| 333 | 3.15 | 21.7 | 333.2 | 0.90 | 2.78 |
| | | | $X_{H_2O} = 0.05$ | 6 | |
| 298 | 3.15 | 69.6 | 298.8 | 0.32 | 0.97 |
| 303 | 3.15 | 56.0 | 303.2 | 0.38 | 1.15 |
| 313 | 3.15 | 37.9 | 313.2 | 0.54 | 1.66 |
| 323 | 3.15 | 27.0 | 323.2 | 0.74 | 2.29 |
| 333 | 3.15 | 20.0 | 333.2 | 0.98 | 3.05 |
| | | | $X_{H_2O} = 0.10$ | 6 | |
| 298 | 3.15 | 54.8 | 298.2 | 0.36 | 1.10 |
| 303 | 3.15 | 44.2 | 303.2 | 0.44 | 1.33 |
| 313 | 3.15 | 30.4 | 313.2 | 0.61 | 1.89 |
| 323 | 3.15 | 22.0 | 323.2 | 0.83 | 2.58 |
| 333 | 3.15 | 16.6 | 333.2 | 1.09 | 3.39 |
| х _{н 2} о =0.185 | | | | | |
| 298 | 3.15 | 50.2 | 298.2 | 0.40 | 1.22 |
| 303 | 3.15 | 40.9 | 303.2 | 0.48 | 1.49 |
| 313 | 3.15 | 28.3 | 313.2 | 0.68 | 2.10 |
| 323 | 3.15 | 20.6 | 323.2 | 0.91 | 2.84 |
| 333 | 3.15 | 15.4 | 333.2 | 1.19 | 3.73 |

ring positions, while peak '4' signals result from the 3- and 4-pyrrolidinium protons. The water 1 H peak at 2.52 ppm is labeled on the spectrum as $H_{2}O$.

The only difference between the 1H spectra of the two water-IL mixtures is the position of the water chemical shift δ_{H_2O} . At the water mole fraction x_{H_2O} =0.1, δ_{H_2O} is 2.44 ppm in Pyrr $_{14}^+$ /NTf $_2^-$ and 3.07 ppm in Pyrr $_{14}^+$ /OTf $_2^-$ at 298.2 K. Water dissolved in the IL associates with the anion $_2^-$. The hydrogen bond strength between water and anion is greater for OTf $_2^-$ than for NTf $_2^-$, which more effectively deshields the proton and shifts δ_{H_2O} further downfield.

Concentration and temperature dependence of δ_0

The chemical shift of water protons, δ_{H_2O} depends on both the water concentration in the IL and on the sample temperature. The chemical shift is a linear function of the ratio of the water mole fraction to the mole fraction of the IL, X_{H_2O}/X_{IL} , over the range of water mole fractions from $X_{H_2O}=0.04-0.18$ for Pyrr $^+_{14}/NTf_2^-$ and from $X_{H_2O}=0.04-0.30$ for Pyrr $^+_{14}/OTf_2^-$. The slopes of the

TABLE IV. Temperature-dependent viscosities (η), ionic conductivities (κ), and molar conductivities (Λ $_{imp}$) for mixtures of Pyrr $_{14}^+$ /OTf $_{-}^-$ and water for the different mole fractions of water, χ_{H_2O} . All uncertainties are identical to those listed in Table III.

| Table | 1111. | | | | |
|---------------------------------|-------|-----------|--------------------|-------------------------------|-----------------------------|
| Tvisc | (K) | η (mPa-s) | Tcond (K) | κ (S-m ⁻¹) | $\Lambda_{imp} \times 10^4$ |
| | | | | | $(S-m^2-mol^{-1})$ |
| | | | $X_{H_2O} = 0.001$ | | |
| 298 | .15 | 168 | 298.2 | 0.20 | 0.46 |
| 303 | .15 | 130 | 303.2 | 0.25 | 0.58 |
| 313 | .15 | 81.6 | 313.1 | 0.37 | 0.88 |
| 323 | .15 | 54.8 | 323.1 | 0.54 | 1.27 |
| 333 | .15 | 38.4 | 333.1 | 0.75 | 1.78 |
| | | | $X_{H_2O} = 0.048$ | | |
| 298 | .15 | 145 | 299.1 | 0.25 | 0.59 |
| 303 | .15 | 113 | 303.1 | 0.30 | 0.70 |
| 313 | .15 | 72.0 | 313.2 | 0.44 | 1.05 |
| 323 | .15 | 48.5 | 323.1 | 0.63 | 1.50 |
| 333 | .15 | 34.4 | 333.1 | 0.86 | 2.05 |
| | | | $X_{H_2O} = 0.117$ | | |
| 298 | .15 | 109 | 298.2 | 0.28 | 0.66 |
| 303 | .15 | 86.3 | 303.2 | 0.35 | 0.82 |
| 313 | .15 | 56.3 | 313.2 | 0.51 | 1.21 |
| 323 | .15 | 39.0 | 323.1 | 0.72 | 1.71 |
| 333 | .15 | 28.2 | 333.1 | 0.97 | 2.32 |
| <i>X</i> _{H 2} 0=0.174 | | | | | |
| 298 | .15 | 92.4 | 298.2 | 0.31 | 0.73 |
| 303 | .15 | 73.5 | 303.2 | 0.38 | 0.90 |
| 313 | .15 | 48.7 | 313.2 | 0.55 | 1.32 |
| 323 | .15 | 34.0 | 323.1 | 0.77 | 1.86 |
| 333 | .15 | 24.8 | 333.1 | 1.04 | 2.52 |

graphs of δ_{H_2O} vs. x_{H_2O}/x_{IL} are 1.97 for Pyrr $^+_{14}/NTf_2^-$ and 1.33 for Pyrr $^+_{14}/OTf_2^-$.

A possible explanation for the dependence of δ_{H_2O} on the water concentration in the IL is the change of proportion between water-water and water-anions bonds with changing water concentration. When the concentration of water is higher, it is more probable for the water molecule to make a bond with another water molecule, leading to a downfield shift. It is worth noting that once the 1 H NMR spectrum of water in a given IL is calibrated, the chemical shift $\delta_{^12O}$ could be used to determine water concentration quite quickly and non-destructively.

We have measured the temperature dependence of δ_{H_2O} for two samples of (Pyrr $_{14}^+$ /NTf $_2^-$)/water mixtures with water concentrations x_{H_2O} = 0.112 and x_{H_2O} = 0.176 and three samples of (Pyrr $_{14}^+$ /OTf $_2^-$)/water mixtures with water concentrations x_{H_2O} = 0.078, x_{H_2O} = 0.126 and x_{H_2O} = 0.204. All measurements were performed for the range of temperatures from 268 K to 318 K. We observed upfield shift of the water peak with increasing temperature. The values of δ_{H_2O} exhibit a linear shift with temperature, as shown on Fig. 5.

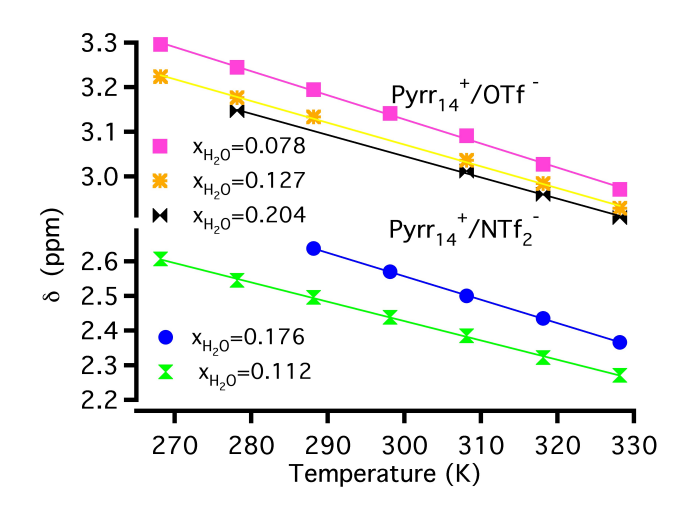


FIG. 5. ¹H NMR chemical shift of H $_2$ O, δ_{H_2O} , in Pyrr $_{14}^+$ /OTf $^-$ (top) and Pyrr $_{14}^+$ /NTf $_2^-$ (bottom).

It is likely that the upfield shift with increasing temperature results from the entropically driven breaking of hydrogen bonds between the water and IL anion, thus leading to an overall decrease of the number of hydrogen bonds per water molecule. This consequentially leads to shielding of proton and upfield shift of the water peak. The same mechanism is reported in literature for bulk water. The temperature dependence of δ_{H_2O} for bulk water is given by δ_{H_2O} = 7.83- T/96.9 (for pH=5.5). In bulk water, the density decreases with increasing temperature, thus leading to fewer and weaker H-bonds. The slopes of the δ_{H_2O} vs. temperature plots are slightly higher for Pyrr $^+_{14}/NTf$ $^-_{2}$ than for Pyrr $^+_{14}/OTf$, and also slightly larger for increasing water concentrations.

= 0.126 and xTemperature dependence of D_{ation} and D_{anion}

The diffusivities were measured for seven samples: three samples of (Pyr $_{H_2O}^{\dagger}$) Water mixtures with water concentrations $X_{H_2O}^{\dagger}$ = 0.00023, X_{H_2O} = 0.112 and X_{H_2O} = 0.176, and four samples of (Pyrr $_{14}^+$ /OTf $^-$)/water mixtures with water concentrations $X_{H_2O} = 0.00065$, $X_{H_2O} = 0.078, X_{H_2O}$ $H_{2}O = 0.204$. For each IL, one sample was kept as dry as possible, namely the $^+_{14}/{\rm NTf}~^-_2$ with x_{H_2O} = 0.00023 and sample of Pyrr $^+_{14}/{\rm OTf}~^-$ with x_{H_2O} = 0.00065. We refer to these low water concentration samples as 'dry'. The temperature dependence of the diffusivities for ILs cations and anions was investigated over the range of temperatures from 278 K to 318 K. Fig. 6 exhibits the temperature dependence for cation diffusivities for all seven samples. The diffusivities are higher for less viscous Pyrr₁₄/NTf ⁻₂ than for Pyrr₁₄/OTf -. Also, a dependence of diffusion on the water concentration in IL is observed. The higher diffusivities are observed for samples with higher water concentration within samples based on the same IL. The full data set for the diffusivities of water, anions and cation in these solutions is given in Fig. 7.

Self-diffusion coefficients for cations and anions of $Pyrr_{14}^+/NTf_2^-$ and $Pyrr_{14}^+/OTf_2^-$ correlate with viscosities

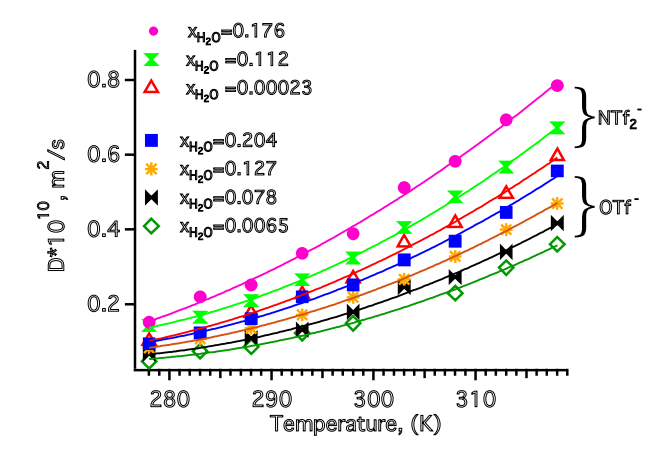


FIG. 6. Temperature dependent diffusivities *D* cation for both IL/water systems; solid lines shown are fits to the VFT equation.

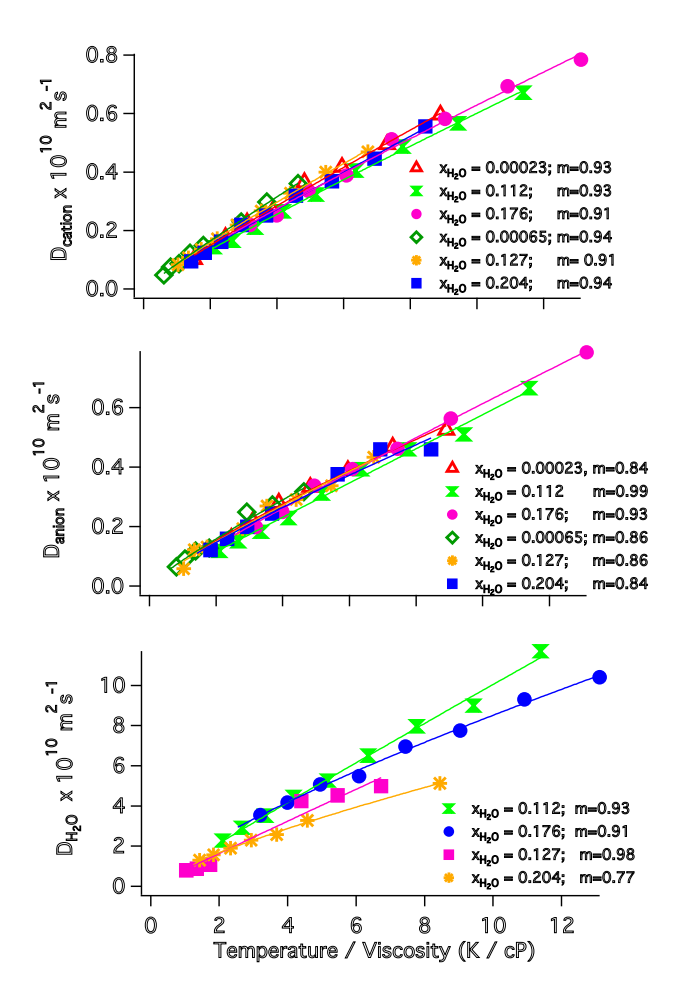


FIG. 7. Self-diffusion coefficients D cation (top), D anion (middle) and D H_2 O (top) plotted vs. the ratio of temperature to viscosity for both IL/water systems. Temperature dependence of the measured pyrrolidinium-ring-proton diffusivities D cation for the IL/water system. The solid lines shown are fits to the FSE model. The red, light green and magenta symbols are for Pyrr $\frac{1}{14}$ /NTf $\frac{1}{2}$ data while the dark green, gold and dark blue symbols are for Pyrr $\frac{1}{14}$ /OTf $\frac{1}{2}$ data. Water mole fractions and FSE exponents m are given in the graph legends.

of these liquids. Ambient temperature viscosities for the IL-water samples show that the increasing values of D_{cation} do scale with the decrease in measured viscosities. Moreno, *et al.* used the PG-SE NMR method to measure the diffusivities and conductivity of Pyrr $^+_{14}/OTf$; after accounting for the differences in water concentrations between the samples they used and our current results, very good agreement is observed.

Ratio of diffusivities Q_{ation} /D $_{anion}$

The anion diffusivities are very similar to those for the cations, with the ratio D cation /D anion being about 1.1 for all samples and temperatures. For Pyrr $_{14}^+/NTf$ $_2^-$, the anion and the cation have very similar values of effective radii: 3.43 and 3.36 Å correspondingly. Therefore, it is unsurprising that the experimental data of D cation /D anion coincide with the predictions from the Stokes-Einstein model. For Pyrr $_{14}^+/OTf$ $_-^-$, the OTf $_-^-$ anion is 1.25 times smaller than the cation, but experimental data for D cation /D anion are also approximately 1.1, as is the case for the Pyrr $_{14}^+/NTf$ $_2^-$. The same trend was observed by other researcher $_-^{40}$: $_-^{13}$ The possible explanation of this phenomenon is the different character of electrostatic interactions with neighboring ions in Pyrr $_{14}^+/OTf$ and Pyrr $_{14}^+/NTf$ $_2^-$.

Friction and transport of H₂O in ILs

It is well known that water and other neutral molecules display faster diffusivity than either cations or anions in ILs. 14,43,44 Kaintz, et al. explored the friction experienced by a range of neutral and charged solutes in IL solutions.43 They found that significantly different friction was observed for charged vs. neutral solutes, as characterized by ξ_{obs}/ξ_{SE} = D_{SE}/D_{obs} , the ratio of the friction observed in PG-SE NMR self-diffusion measurements to the friction calculated from the Stokes-Einstein (SE) equation. This trend is for this ratio to be larger than unity for charged solutes and less than unity for neutral solutes.43 The deviations from unity in this ratio ξ_{obs}/ξ_{SE} are greater when the solute is small, with a roughly linear trend observed in the friction ratio when plotted against the ratio of van der Waals volumes for the solute to the solvent, V_u/V_v , where the IL volume is taken to be the average of the anionic and cationic volumes.43

We can compare our results for the diffusivity of water in ILs with those reported by Kaintz, et al. for larger and more hydrophobic species by considering their summary graph of ξ_{obs}/ξ_{SE} vs. V_u/V_v , given as Fig. 9 of ref. 43. The van der Waals volume of water can be taken to be 20.6 Å³. Since the van der Waals volumes of our anions are V(OTf $^-$)=85.9 and V(NTf $^-_2$)=158.7Å³ and the cationic volume is V(Pyrr $^+_{14}$)=169.0 Å³, 43 we average the anionic and cationic volumes to obtain IL volumes of V(Pyrr $^+_{14}$ /OTf $^-$)= 127.5 and V(Pyrr $^+_{14}$ /NTf $^-_2$)=163.9 Å³. This leads to volume ratios of the water solute to the IL of V_u/V_v =0.126 for Pyrr $^+_{14}$ /OTf $^-$ and V_u/V_v =0.62 for Pyrr $^+_{14}$ /NTf $^-_2$. Using the measured temperatures,

viscosities and water diffusivities for our solutions, we find that the friction ratios $\xi_{obs}/\xi_{SE} = D_{SE}/D_{obs}$ are in the range from 0.039 to 0.045 for solutions of water in Pyrr $_{14}^+/NTf_{2}^-$ and in the range of 0.045 to 0.071 for Pyrr $_{14}^+/OTf_{2}^-$. Simply put, our values lie significantly to the left of the trend line shown in Fig. 9 of ref. 43. Our friction ratios for water diffusivity are a factor of 2 lower for Pyrr $_{14}^+/NTf_{2}^-$ and a factor of three lower for Pyrr $_{14}^+/OTf_{2}^-$ than would be predicted by the trends shown for neutral solutes in ILs discussed by Kaintz, *et al.*⁴³

The mechanism for understanding such differences in local friction for water relative to the IL anions cation are explored in an elegant study by Araque, al.44 Among the things reported in set of molecular dynamics simulations is a study of the transport of the isoelectronic pair methane and the ammonium cation in the Pyrr ⁺₁₄/NTf ⁻₂ IL. Araque, et al. show that methane is solubilized in regions that are rich in the non-polar butyl tails of the Pyrr 14 cation, which can be characterized as being locally "softer", or lower friction, as a result of decreased electrostriction. Ammonium is localized in the more polar regions of the Pyrr ⁺₁₄/NTf ⁻₂ IL that are "stiffer" and have higher friction because of electrostriction. The polar, higher friction regions lead to increased local caging and slower diffusivity of the charged ammonium solute, while the lower polarity regions with lower friction show less caging and approximately an order of magnitude increase in diffusive jumps between local cages⁴⁴ We can presume that water will also avoid the apolar regions of Pyrr 14/NTf 2 and display increased diffusive jumps relative to the IL anions and cations. However, the water transport will also be modulated by the strong H-bonding interactions between water and the anions as well as between water molecules.

Other recent results point to the significant differences between neutral vs. charges solutes in ILs. Recently, Liang, et al. reported that the diffusivity of deuterated hexane in solutions of the P $^+_{14,666}$ /NTf $^-_2$ IL is on average 21 times larger than for the cation. 45 Sarraute, et al. reported the diffusivities of several of the 1-alkyl-3methylimidazolium NTf 2 ILs at infinite dilution in water, methanol and acetonitrile; strong specific interactions were observed between the IL anions and cations and the water.46 These strong, specific hydrogen-bonding interactions were studied in detail by Kramer, et al. using 2D-IR spectroscopy.47 Their results showed that the dynamics of the water hydroxyl stretch are affected by a broad distribution of timescales for non-exponential relaxation of both the strength of the hydrogen bonds between water and anions and the orientational relaxation of the water hydroxyl group. 47 This picture is fully consistent with the broad and heterogeneous timescales for both solvation dynamics 48 and chemical reactions in ILs. 49-51

Ratio of D H2O to D cation

The molecular volume of the Pyrr $_{14}^{+}$ cation is 8 times larger than that for water. Thus, if Stokes-Einstein hydrodynamic predictions were meaningful, we would expect to see a ratio of hydrodynamic radii being approximately 2, with similar scaling for the diffusivities. Clearly this will not be the case, since the frictional forces affecting translation of the neutral water will be much different than for the anions and cations.

This ratio D_{H_2O}/D_{cation} was different for the two ionic liquids that we investigated. It was $D_{H_2O}/D_{cation} = 20$ for hydrophobic Pyrr $_{14}^+/NTf_2^-$ and $D_{H_2O}/\bar{D}_{cation}$ =15 for less hydrophobic and more water miscible Pyrt₄/OTf ⁻ These differences can be explained by different microviscosities experienced by water molecules in Pyrt₄/NTf ₂ relative to Pyrr ⁺₁₄/OTf ⁻. Interactions between water molecules and anions are different for hydrophobic NT\$\overline{t}\$ vs. the more water miscible OTf anions, which is consistent with the observation that δ_{H_2O} is shifted further downfield for water dissolved in Pyrr 14/OTf - compared to water dissolved in Pyrr₁₄/NTf ⁻₂ . Fig. 8 shows that the ratio D H2O/D cation decreases with increasing temperature for both ILs. Over our observed temperature range between 278 to 318 K, the thermal energy of the system increases by only 15% However, our observed changes in transport ratios for water relative to cation change by a much larger value. Vibrational spectroscopy informs us that the H-bond interaction is stronger between water to the OTf $\bar{}$ anion than to the NTf $\bar{}$ anion.^{7,8}

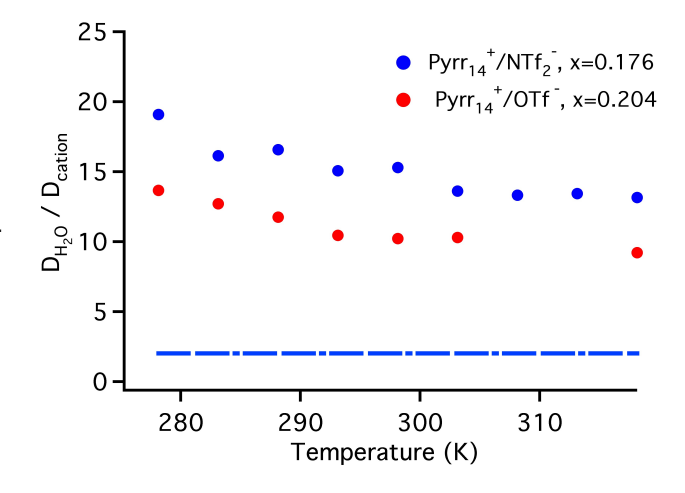


FIG. 8. Temperature dependence of the ratio of diffusivities for water to cation, $D_{H_2O/D}$ cation . The dot-dashed line indicated the ratio of 2 for $D_{H_2O/D}$ cation predicted by the Stokes-Einstein hydrodynamic model.

Activation energies for diffusivity

While a VFT model provides the best fit to the diffusivity data, it is still useful to consider the high-temperature Arrhenius limit. Activation energies E_a for diffusion of anions, cations and water were calculated from a log plot of diffusion coefficients vs. inverse temperature and are presented in Table V. As expected, activation energies of diffusion are smaller for less viscous

Pyrr $_{14}^+$ /NTf $_2^-$ than for Pyrr $_{14}^+$ /OTf $_-$. The values of E_a for anionic and cationic diffusivity are reduced for samples with larger water concentration. Strong correlations are observed between the Arrhenius activation energy for the shear viscosity and the cationic diffusivity. The activation energy for water transport is significantly less than the values for either anionic or cationic diffusivity, but is at least 2.5 times larger than a typical value for the enthalpy of water-water hydrogen bonds. This indicates that the water is likely to be interacting strongly with the IL anions, not just other water molecules, even at the highest concentrations of X_{H_2O} =0.176 and 0.204 for NTf $_2^-$ and OTf $_2^-$ anions, respectively.

TABLE V. Arrhenius enthalpies E $_a$ for diffusivities obtained from PG-SE NMR data, in units of kJ mol $^{-1}$. The estimated uncertainty in the E $_a$ is ± 2 kJ mol $^{-1}$.

| X _{H₂O} | E _a (cation) | E _a (anion) | E a (H ₂ O)) | | | |
|---|--|------------------------|-------------------------|--|--|--|
| | Pyrr ⁺ ₁₄ /NTf ⁻ ₂ | | | | | |
| 0.00023 | 32.2 | 30.8 | - | | | |
| 0.112 | 30.0 | 31.7 | 29.3 | | | |
| 0.176 | 29.8 | 30.4 | 23.3 | | | |
| Pyrr ⁺ ₁₄ /OTf ⁻ | | | | | | |
| 0.00065 | 35.8 | 34.2 | - | | | |
| 0.078 | 34.0 | 34.5 | - | | | |
| 0.127 | 32.0 | 32.4 | _ | | | |
| 0.204 | 31.8 | 32.2 | 25.3 | | | |

The Stokes-Einstein hydrodynamic model predicts slower diffusion than was observed. Our diffusivity measurements directly assess the friction experienced by the cations, the anions and the water molecules in our samples. While van der Waals interactions and molecular size do affect transport properties, the larger contributions to the friction for our water-IL solutions are determined by Coulombic and specific H-bonding effects between the ions and water.

lonicity of ILs as a function of water content and temperature

Work from the Hayamizu and Watanabe groups has shown that we can fruitfully consider the degree of ionicity for an ionic liquid by considering the ratio of conductivity to a calculated conductivity obtained from the NMR PG-SE experiments. 10,11,34–36 The conductivity is measured experimentally by impedance methods. The NMR conductivity is calculated from

$$\Lambda_{NMR} = F^{2} (D_{anion} + D_{cation}) / (RT),$$
 (5)

where F is the Faraday constant.³⁴ The ionicity parameter is then calculated from the ratio of $\Lambda_{mpedance}$ / Λ_{NMR} .

When paired with the ${\rm NTf}_2^-$ anion, ILs having the Pyrr $_{14}^+$ cation are known to exhibit a greater ionicity than other ILs with similarly sized aromatic cations such as bmim $^+$ or 1-butylpyridinium or butyltrimethylammonium. 36 Tokuda, *et al.* showed that

for the bmim $^+$ /NTf $_2^-$ and bmim $^+$ /OTf $^-$ ILs, the ionicity parameters are 0.57 and 0.63, respectively. They also report an ionicity parameter of 0.70 for Pyrr $_{14}^+$ /NTf $_2^-$. 36 Mbondo Tsamba, $et\ al.$ show that for the set of four ILs pairing emim $^+$ and bmim $^+$ cations with CH $_3$ OSO $_3^-$ and OTf $^-$ anions, the ionicity decreases sharply with increasing temperature over the range from 298 to 343 K. Increasing the cationic alkyl chain length from ethyl to butyl decreases the 298 K ionicity from 0.68 to 0.60 for emim $^+$ /OTf $^-$ and bmim $^+$ /OTf $^-$, respectively. 39

lonicity in neat ILs is less complex than for the case of ILs with added water. The limited ionicity data given in Table VI show fluctuations in the ionicity with changes in water content. While the ionicity of neat ILs decreases significantly on warming the samples from 298 to 313 K, 39 this does not occur for IL-water mixtures. Previously, Andanson, *et al.* studied the effect of water addition on the ionicity of the two ILs pairing the emim $^+$ and bmim $^+$ cations with the methylsulfate anion. Andanson, *et al.* observed that changes to the ionicity are only observable for samples with the highest water content above $x_{H_2O} > 0.8$. Since the water concentrations in ILs that we have studied here are much lower, we conclude that this is the reason for the apparent lack of effect on the observed ionicities.⁵²

TABLE VI. Ionicity (Λ imp / Λ NMR) as a function of water concentration and temperature. Estimated uncertainties in the ionicity values are $\pm 5\%$.

| , | | | |
|---------|------------------|--|--------------------|
| | | Pyrr ⁺ ₁₄ /NTf ⁻ ₂ | |
| T (K) x | $H_2o = 0.00023$ | $X_{H_2O} = 0.112$ | $X_{H_2O} = 0.176$ |
| 298 | 0.81 | 0.84 | 0.76 |
| 303 | 0.75 | 0.81 | 0.75 |
| 313 | 0.80 | 0.85 | _ |
| | | Pyrr ⁺ ₁₄ /OTf ⁻ | |
| T (K) x | $H_2o = 0.00065$ | $X_{H_2O} = 0.127$ | $X_{H_2O} = 0.204$ |
| 298 | 0.87 | 0.83 | 0.74 |
| 303 | - | 0.79 | _ |
| 313 | 0.82 | 0.86 | 0.77 |
| | | | |

Temperature dependence of the water diffusivity

Self-diffusion of water in ILs is substantially faster than expected based on hydrodynamic predictions and is much faster than the anionic or cationic diffusivities. The temperature dependence for water diffusivity in the ILs is shown in Fig. 9. The smaller size of the water molecule relative to the anions and cation leads to a Stokes-Einstein prediction of water diffusivity that should be 2 times faster than either the anion or cation. However, the observed water diffusivity 10–20 times faster. Anomalously high diffusivity of water dissolved in ILs was also reported by other researchers.

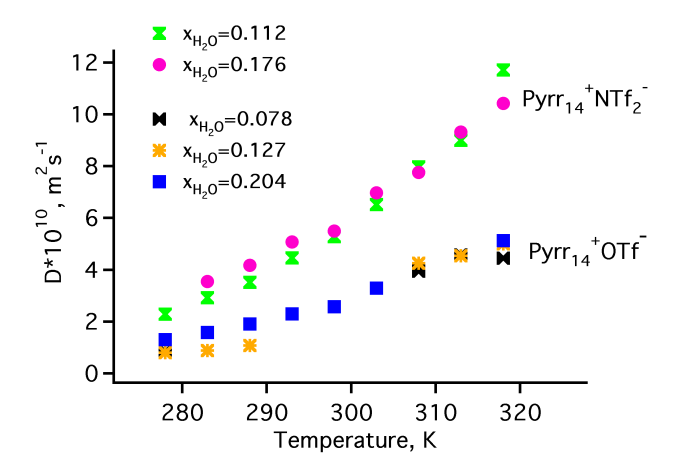


FIG. 9. Temperature dependence of the water proton diffusivity D_{H_2O} in the IL/water system.

Fractional Stokes-Einstein behavior of the cation, anion and water diffusivities.

Harris showed that a number of liquids often display fractional Stokes-Einstein (FSE) behavior, where the diffusivity scales as $D \sim (T/\eta)^m$, where $m \le 1$. These liquids include several neutral solvents, fragile glassformers, and other soft matter systems such as ionic liquids. For several ILs with dialkylimidazolium cations and BF $_4^-$ or PF $_6^-$ anions, the FSE exponent m = 0.90.54

Our diffusivity studies of the two ILs Pyrr₁₄/NTf ⁻₂ and Pyrr ⁺₁₄/OTf ⁻ and with added water show FSE behavior as illustrated in Fig. 7 by the graphs of D plotted vs. T/η . Normal Stokes-Einstein hydrodynamics would require a linear plot; FSE behavior is indicated by the deviation from linearity. The FSE exponents m for the Pyrr $_{14}^+$ cation are clustered about the value m=0.93. The FSE exponents for anion diffusivity are more broadly distributed in the range from 0.84 to 0.99, with the values of m for the NTf $\frac{1}{2}$ anion being higher than for the OTf anion. A similar distribution is seen for the water diffusivity. As discussed above, the uncertainties for the water diffusivities are larger, in part because of the lower concentrations, and also because the faster ¹H diffusion signal for water must be deconvolved from the larger amplitude signals for the Pyrr ⁺₁₄ cation.

CONCLUSIONS

We have fully characterized the temperature transport properties for several mixtures of water with the two ILs Pyrr $_{14}^+$ /NTf $_2^-$ and Pyrr $_{14}^+$ /OTf $_-^-$. One of the most striking results is that the ratio of water diffusivity is 10–20 times larger than that of the Pyrr $_{14}^+$ cation. The observation that the ratio D_{H_2O}/D_{cation} ranges between 10–20 indicates that hydrodynamic descriptions cannot be useful on the molecular scale. Temperature-dependent diffusivities show fractional Stokes-Einstein behavior with an FSE exponent m in the range from 0.84 to 1.Another intriguing result is that the ratio of water diffusivity to

cation diffusivity decreases with increasing temperature for both ILs studied, Pyrr $_{14}^+/NTf$ $_2^-$ and Pyrr $_{14}^+/OTf$ $_-^-$. A significant difference between the two ILs is that the hydrophobic IL Pyrr $_{14}^+/NTf$ $_2^-$ phase separates from water, whereas the IL with the OTf $_-^-$ anion is water miscible. The notable result is that the ratio of diffusivity of water to cation is significantly larger for Pyrr $_{14}^+/NTf$ $_2^-$ vs. Pyrr $_{14}^+/OTf$ $_-^-$. It is therefore important that transport of water and other neutral species in IL solutions be measured carefully, as simple hydrodynamic predictions will not apply.

During the course of this work we have considered two spectroscopic methods for non-destructively determining the water content that were calibrated against the standard Karl-Fischer titrations. While ¹H NMR can be useful in certain circumstances, vibrational spectroscopy of the water combination band at 5,250 cm ⁻¹ provides a similar detection limit for water as the KF titrations while leaving the sample intact. The fact that careful FT-IR and NMR measurements of water content in ILs will permit more rapid generation of novel ILs having very high purity levels.

The interactions between neutral solutes or co-solvents in ionic liquid solutions are complex. For hydrophobic and non-hydrogen-bonding species, the interactions will be primarily a result of van der Waals forces. For water, the presence of strong H-bond donation from the water to the anion leads to interactions that can be as strong as or stronger than anion-cation interactions. We anticipate that the data presented here will be further tested by detailed molecular simulations. A broad understanding of water in ILs can be compared with the properties of other neutral co-solvents and small solutes. Hopefully this knowledge will accelerate the use of ILs for a broad range of applications to energy technologies.

ACKNOWLEDGMENTS

TAF and EWC gratefully acknowledge support for the work at Rutgers from the National Science Foundation on grant number CHE-1362272. JAD thanks the Rutgers Aresty Undergraduate Research Foundation for support. SGG acknowledges support from the Office of Naval Research. We thank Dr. Seho Kim and Dr. Nagarajan Murali (Rutgers) for their invaluable help with the NMR measurements, and Dr. James F. Wishart (Brookhaven) for helpful discussions and comments on the manuscript. PH and MCG wish to acknowledge the financial support of the Contrat d'Objectifs Partag´es, CNRS-UBP-R´egion Auvergne, France.

¹D. R. MacFarlane, M. Forsyth, P. C. Howlett, J. M. Pringle, J. Sun, G. Annat, W. Neil, and E. I. Izgorodina, "lonic liquids in electrochemical devices and processes: managing interfacial Electrochemistry," Acc. Chem. Res., 40, 1165 (2007).

²M. Armand, F. Endres, D. R. MacFarlane, H. Ohno, and B. Scrosati, "lonic-liquid materials for the electrochemical challenges of the future," Nat. Mater., 8, 621 (2009).

³M. G. Freire, A. F. M. Claudio, J. M. M. Araujo, J. A. P. Coutinho, I. M. Marrucho, J. N. C. Lopes, and L. P. N. Rebelo,

- "Aqueous biphasic systems: a boost brought about by using ionic liquids." Chem. Soc. Rev., 41, 4966 (2012).
- ⁴R. P. Swatloski, J. D. Holbrey, and R. D. Rogers, "lonic liquids are not always green: hydrolysis of 1-butyl-3-methylimidazolium hexafluorophosphate," Green Chemistry, 5, 361 (2003).
- ⁵C. Li, B. Knierim, C. Manisseri, R. Arora, H. V. Scheller, M. Auer, K. P. Vogel, B. A. Simmons, and S. Singh, "Comparison of dilute acid and ionic liquid pretreatment of switchgrass: Biomass recalcitrance, delignification and enzymatic saccharification," Bioresour. Technol., 101, 4900 (2010).
- ⁶ J. Jacquemin, P. Husson, A. A. H. Padua, and V. Majer, "Density and viscosity of several pure and water-saturated ionic liquids," Green Chem., **8**, 172 (2006).
- ⁷L. Cammarata, S. Kazarian, P. Salter, and T. Welton, "Molecular states of water in room temperature ionic liquids," Phys. Chem. Chem. Phys., 3, 5192 (2001).
- ⁸C. D. Tran, S. H. De Paoli Lacerda, and D. Oliveira, "Absorption of Water by Room-Temperature Ionic Liquids: Effect of Anions on Concentration and State of Water," Appl. Spectrosc., 57(2), 152 (2003).
- ⁹K. R. J. Lovelock, A. Deyko, P. Licence, and R. G. Jones, "Vaporisation of an ionic liquid near room temperature," Phys. Chem. Chem. Phys., 12, 8893 (2010).
- 10 H. Tokuda, K. Hayamizu, K. Ishii, M. A. B. H. Susan, and M. Watanabe, "Physicochemical Properties and Structures of Room Temperature Ionic Liquids.
 Length in Imidazolium Cation," J. Phys. Chem. B, 109, 6103 (2005).
- ¹¹H. Tokuda, S. Tsuzuki, M. A. B. H. Susan, K. Hayamizu, and M. Watanabe, "How Ionic Are Room-Temperature Ionic Liquids? An Indicator of the Physicochemical Properties," J. Phys. Chem. B, 110, 19593 (2006).
- ¹²A. Wulf, K. F. D. Michalik, and R. Ludwig, "IR and NMR Properties of Ionic Liquids: Do They Tell Us the Same Thing?" ChemPhysChem, 8, 2265 (2007).
- ¹³A. Menjoge, J. Dixon, J. Brennecke, E. Maginn, and S. Vasenkov, "Influence of Water on Diffusion in Imidazolium-Based Ionic Liquids: A Pulsed Field Gradient NMR study," J. Phys. Chem. B, 113, 6353 (2009).
- ¹⁴ J. Hou, Z. Zhang, and L. A. Madsen, "Cation/Anion Associations in Ionic Liquids Modulated by Hydration and Ionic Medium," J. Phys. Chem. B, 115, 4576 (2011).
- ¹⁵ M. Moreno, M. Montanino, M. Carewska, G. Appetecchi, S. Jeremias, and S. Passerini, "Water-soluble, triflate-based, pyrrolidinium ionic liquids," Electrochimica Acta, 99, 108 (2013).
- ¹⁶ E. O. Stejskal, "Use of spin echoes in a pulsed magnetic-field gradient to study anisotropic, restricted diffusion and flow," J. Chem. Phys., 43, 3597 (1965).
- ¹⁷ J. E. Tanner, "Use of the stimulated echo in NMR diffusion studies," Journal of Chemical Physics, 52 (5), 2523 (1970).
- ¹⁸ D. Wu, A. Chen, and C. S. J. Johnson, "An Improved Diffusion Ordered Spectroscopy Experiment Incorporating Bipolar Gradient Pulses," J. Magn. Reson., A115, 260 (1995).
- ¹⁹ F. Castiglione, M. Moreno, G. Raos, A. Famulari, A. Mele, G. B. Appetecchi, and S. Passerini, "Structural Organization and Transport Properties of Novel Pyrrolidinium-Based Ionic Liquids with Perfluoroalkyl Sulfonylimide Anions," J. Phys. Chem. B, 113, 10750 (2009).
- ²⁰Y. Lingscheid, S. Arenz, and R. Giernoth, "Heteronuclear NOE Spectroscopy of Ionic Liquids." ChemPhysChem, 15, 261 (2012).
- ²¹ H. Y. Lee, H. Shirota, and E. W. Castner, Jr., "Differences in Ion Interactions for Isoelectronic Ionic Liquid Homologs," J. Phys. Chem. Lett., 4, 1477 (2013).
- ²²S. Khatun and E. W. Castner, Jr., "Ionic Liquid-Solute Interactions Studied by 2D NOE NMR Spectroscopy," J. Phys Chem. B, ASAP (2014), doi:10.1021/jp509861g.
- ²³C. E. S. Bernardes, M. E. Minas da Piedade, and J. N. Canongia Lopes, "The Structure of Aqueous Solutions of a Hydrophilic Ionic Liquid: The Full Concentration Range of 1-Ethyl-3-methylimidazolium Ethylsulfate and Water," J. Phys. Chem.

- B, 115, 2067 (2011).
- ²⁴W. A. Henderson, V. G. Young, W. Pearson, S. Passerini, H. C. De Long, and P. C. Trulove, "Thermal phase behaviour of N-alkyl-N-methylpyrrolidinium and piperidinium bis(trifluoromethanesulfonyl)imide salts," J. Phys.: Condens. Matter, 18, 10377 (2006).
- ²⁵W. A. Henderson, M. Herstedt, V. G. Young, S. Passerini, H. C. De Long, and P. C. Trulove, "New Disordering Mode for TFSI-Anions: The Nonequilibrium, Plastic Crystalline Structure of Et4NTFSI," Inorg. Chem., 45, 1412 (2006).
- ²⁶ A. Andresova, J. Storch, M. Tra ikia, Z.Wagner, M. Bendova, and P.Husson, "Branched and cyclic alkyl groups in imidazolium-based ionic liquids: molecular organization and physico-chemical properties," Fluid Phase Equilib., 37, 41 (2014).
- ²⁷T. D. W. Claridge, *High-Resolution NMR Techniques in Organic Chemistry* (Elsevier, 2009).
- 28 (See supplemental material at _____ for more detailed information on measurements of density, viscosity, conductivity, and FT-IR spectra.).
- ²⁹ V. Ananikov, "Characterization of Molecular Systems and Monitoring of Chemical Reactions in Ionic Liquids by Nuclear Magnetic Resonance Spectroscopy," Chemical Reviews, 111, 41 (2011)
- ³⁰ H. E. Gottlieb, V. Kotlyar, and A. Nudelman, "NMR Chemical Shifts of Common Laboratory Solvents as Trace Impurities," J. Org. Chem., 62, 7512 (1997).
- 31T. A. Fadeeva, Probing Local Environments in Ionic Liquids, Ph.D. thesis, Rutgers, The State University of New Jersey (2011).
- ³²F. Gacino, T. Regueira, L. Lugo, M. Comunas, and J. Fernandez, "Influence of Molecular Structure on Densities and Viscosities of Several Ionic Liquids," J. Chem. Eng. Data, 56, 4984 (2011).
- ³³ K. R. Seddon, A. Stark, and M.-J. Torres, "Influence of chloride, water, and organic solvents on the physical properties of ionic liquids," Pure Appl. Chem., 72, 2275 (2000).
- ³⁴ A. Noda, K. Hayamizu, and M. Watanabe, "Pulsed-Gradient Spin-Echo ¹ H and ¹⁹ F NMR Ionic Diffusion Coefficient, Vis cosity, and Ionic Conductivity of Non-Chloroaluminate Room-Temperature Ionic Liquids," J. Phys. Chem. B, **10**5, 4603 (2001).
- ³⁵ H. Tokuda, H. Kikuko, K. Ishii, M. A. B. H. Susan, and M. Watanabe, "Physicochemical Properties and Structures of Room Temperature Ionic Liquids. 1. Variation of Anionic Species," J. Phys. Chem. B, 108, 16593 (2004).
- ³⁶ H. Tokuda, K. Ishii, M. A. B. H. Susan, S. Tsuzuki, K. Hayamizu, and M. Watanabe, "Physicochemical Properties and Structures of Room-Temperature Ionic Liquids. 3. Variation of Cationic Structures," J. Phys. Chem. B, 110, 2833 (2006).
- ³⁷ A. M. Funston, T. A. Fadeeva, J. F. Wishart, and E. W. Castner, Jr., "Fluorescence Probing of Temperature-Dependent Dynamics and Friction in Ionic Liquid Local Environments," J. Phys. Chem. B, 111, 4963 (2007).
- ³⁸ F. S. Oliveira, M. G. Freire, P. J. Carvalho, J. A. P. Coutinho, J. N. C. Lopes, L. P. N. Rebelo, and I. M. Marrucho, "Structural and Positional Isomerism Influence in the Physical Properties of Pyridinium NTf2-Based Ionic Liquids: Pure and Water-Saturated Mixtures," Journal of Chemical & Engineering Data, 55, 4514 (2010).
- ³⁹ B. E. M. Tsamba, S. Sarraute, M. Tra¨ıkia, and P. Husson, "Transport Properties and Ionic Association in Pure Imidazolium- Based Ionic Liquids as a Function of Temperature," J. Chem. Eng. Data, 59, 1747 (2014).
- ⁴⁰ M. Vranes, S. Dozic, and S. Gadzuric, "Physicochemical Characterization of 1-Butyl-3-methylimidazolium and 1-Butyl-1-methylpyrrolidinium Bis(trifluoromethylsulfonyl)imide," J. Chem. Eng. Data, 57, 1072 (2012).
- ⁴¹K. R. Harris, L. A. Woolf, M. Kanakubo, and T. Ruther, "Transport Properties of N-Butyl-methylpyrrolidinium Bis(trifluomethylsulfonyl)amide," J.Chem. Eng. Data, 56, 4672 (2011).
- ⁴² J. Cavanagh, W. J. Fairbrother, A. G. Palmer, Protein NMR Spectroscopy (Academic Press, San Diego, CA,

1996).

- ⁴³ A. Kaintz, G. Baker, A. Benesi, and M. Maroncelli, "Solute Diffusion in Ionic Liquids, NMR Measurements and Comparisons to Conventional Solvents," The Journal of Physical Chemistry B, 117, 11697 (2013).
- ⁴⁴ J. C. Araque, S. K. Yadav, M. Shadeck, M. Maroncelli, and C. J. Margulis, "How Is Diffusion of Neutral and Charged Tracers Related to the Structure and Dynamics of a Room-Temperature Ionic Liquid? Large Deviations from Stokes-Einstein Behavior Explained," J. Phys. Chem. B, 119, 7015 (2015), pMID: 25811753.
- ⁴⁵ M. Liang, S. Khatun, and E. W. Castner, "Communication: Unusual structure and transport in ionic liquid-hexane mixtures," The Journal of Chemical Physics, 142, 121101 (2015).
- ⁴⁶S. Sarraute, M. F. Costa Gomes, and A. A. H. Pádua, "Diffusion Coefficients of 1-Alkyl-3-methylimidazolium Ionic Liquids in Water, Methanol, and Acetonitrile at Infinite Dilution," Journal of Chemical & Engineering Data, 54, 2389 (2009).
- ⁴⁷P. L. Kramer, C. H. Giammanco, and M. D. Fayer, "Dynamics of water, methanol, and ethanol in a room temperature ionic liquid," The Journal of Chemical Physics, 142, 212408 (2015).
- ⁴⁸ X.-X. Zhang, M. Liang, N. P. Ernsting, and M. Maroncelli, "Complete Solvation Response of Coumarin 153 in Ionic Liquids," Journal of Physical Chemistry B, 117, 4291 (2013).

- ⁴⁹ X. Li, M. Liang, A. Chakraborty, M. Kondo, and M. Maroncelli, "Solvent-Controlled Intramolecular Electron Transfer in Ionic Liquids," J. Phys. Chem. B, 115, 6592 (2011).
- ⁵⁰ M. Liang, A. Kaintz, G. A. Baker, and M. Maroncelli, "Bi-molecular Electron Transfer in Ionic Liquids: Are Reaction Rates Anomalously High?" Journal of Physical Chemistry B, 116, 1370 (2012).
- ⁵¹H. Y. Lee, J. B. Issa, S. S. Isied, E. W. Castner, Jr., Y. Pan, C. L. Hussey, K. S. Lee, and J. F. Wishart, "A Comparison of Electron-Transfer Dynamics in Ionic Liquids and Neutral Solvents," J. Phys. Chem. C, 116, 5197 (2012).
- ⁵² J.-M. Andanson, M. Tra ikia, and P. Husson, "Ionic association and interactions in aqueous methylsulfate alkyl-imidazoliumbased ionic liquids," The Journal of Chemical Thermodynamics, 77, 214 (2014).
- ⁵³ A.-L. Rollet, P. Porion, M. Vaultier, I. Billard, M. Deschamps, C. Bessada, and L. Jouvensal, "Anomalous Diffusion of Water in [BMIM][TFSI] Room-Temperature Ionic Liquid," J. Phys. Chem. B, 111, 11888 (2007).
- ⁵⁴ K. R. Harris, "The Fractional Stokes-Einstein Equation: Application To Lennard-Jones, Molecular, And Ionic Liquids," J. Chem. Phys., 131, 54503 (2009).